Available online at www.sciencedirect.com
SCIENCE DIRECT®
Journal of Sound and Vibration 283 (2005) 1163–1179
JOURNAL OF SOUND AND VIBRATION
www.elsevier.com/locate/jsvi

Short Communication

Analysis of time-varying rolling element bearing characteristics

Hoon-Voon Liew[a], Teik C. Lim[b,*]

[a] *University of Alabama, Department of Mechanical Engineering, 290 Hardaway Hall, Box 870276, Tuscaloosa, AL 35487-0276, USA*

[b] *University of Cincinnati, Mechanical, Industrial and Nuclear Engineering, 598 Rhodes Hall, P.O. Box 210072, Cincinnati, OH 45221-0072, USA*

Received 9 June 2004; accepted 16 June 2004

1. Introduction

This paper extends the rolling element bearing stiffness matrix formulation developed by Lim and Singh [1–5] to include the time-variation effect of raceway rotation. In that earlier work, the rolling element bearing stiffness matrix was formulated in time-invariant form assuming fixed element position. However, due to the orbital motion of the elements under most rotating conditions, the true nature of the bearing stiffness is periodic in time. Characterizing the time-varying form of the stiffness function, and computing its impact on the vibration response of geared rotor system is the focus of this communication.

The first few major works on rolling element bearing were performed by Jones [6], Harris [7], and Palmgren [8]. They described the radial and axial load-deflection behavior using a nonlinear stiffness coefficient, which were subsequently adopted in numerous bearing analyses [9–11]. However, these early bearing stiffness models were inadequate and incapable of predicting the vibration transmission across bearings. To address the problem, a more generalized formulation based on the Hertzian theory, which relates the raceway displacement vector to the bearing load vector, was formulated by Lim and Singh [1–5]. The new theory led to the derivation of a time-invariant bearing stiffness matrix $[K]_{bm}$ of dimension 5 corresponding to 2 radial, 1 axial, and 2 angular coordinates; the rotation about the shaft axis by design is free. This new bearing stiffness

*Corresponding author. Tel.: +1 513 556 4450; fax: +1 513 556 3390.
E-mail address: teik.lim@uc.edu (T.C. Lim).

0022-460X/$ - see front matter
doi:10.1016/j.jsv.2004.06.022

theory was further applied to examine bearing systems in rotor and geared machineries [2–4]. In another study, Houpert [12] proposed a comparable set of nonlinear algebraic equations relating the 3 bearing forces and 2 tilting moments to the displacement vector and design parameters. The work simply produced a time-invariant nonlinear bearing element for structural analysis of systems with shafts, bearings and housing. Also, Houpert's theory fell short of providing an explicit stiffness matrix that can be used for vibration transmissibility.

2. Time-varying stiffness

The basic assumptions and nomenclature employed by Lim and Singh [1–5] in the earlier studies are adopted here unless indicated otherwise. For reference, Fig. 1 shows the ball and roller

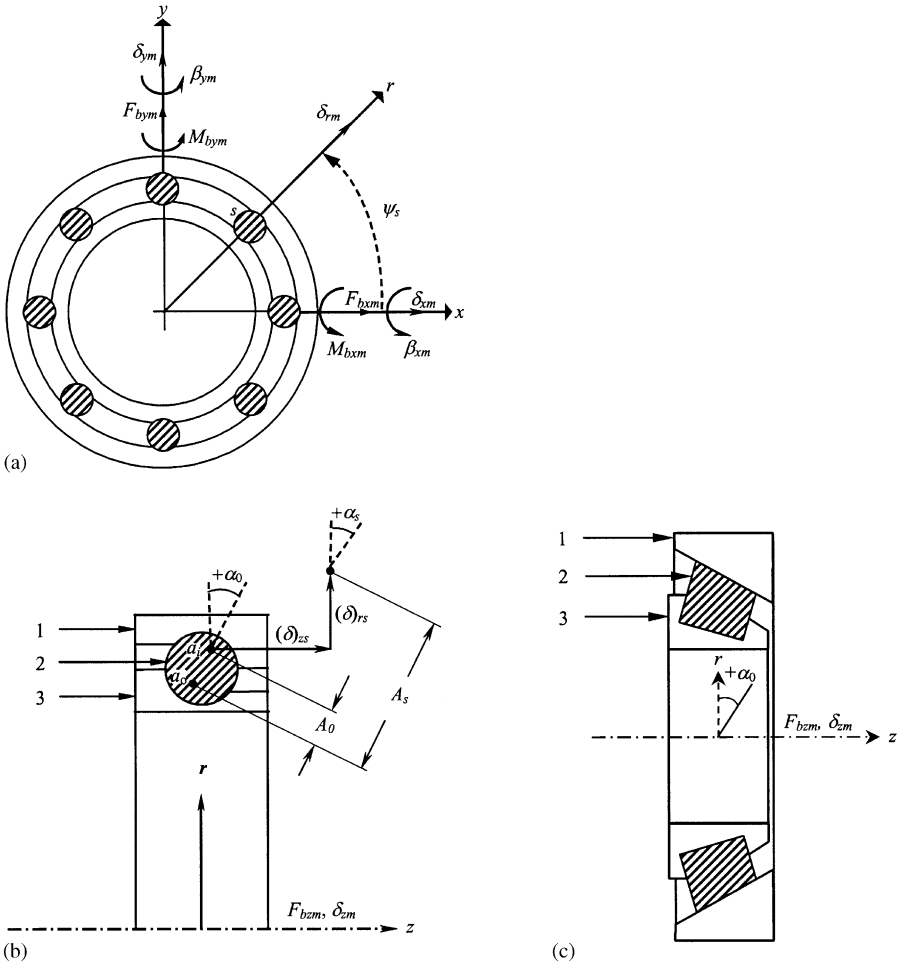

Fig. 1. Rolling element bearing kinematics and the corresponding coordinate systems: (a) radial view; (b) axial view of ball bearing; (c) axial view of roller bearing; outer ring (cup), 1; rolling element, 2; inner ring (cone), 3.

bearing kinematics and their corresponding coordinate systems employed here. The Hertzian theory is applied to describe the elastic contacts between the rolling elements and raceways (i.e. cup and cone).

To track the movement of the rolling elements, we can define the instantaneous orbital position angle ψ_s of the sth element at time t from the pre-defined x-axis assuming pure rolling as

$$\psi_s(t) = \frac{1}{2}\left(1 - \frac{r_b}{r_d}\cos(\alpha_0)\right)\Omega_z t + \frac{2\pi(s-1)}{Z}, \quad s = 1, 2, \ldots, Z. \tag{1}$$

where r_b is the element radius, α_0 is the unloaded contact angle, Ω_z is the mean shaft rotational speed, r_d is the inner race curvature center radius for ball type or pitch radius for roller type, and Z is the number of elements. Due to the orbital rotation Ω_z, the number and position of each element under stress will vary with time as shown qualitatively in Figs. 2(a) and (b) that depict two snapshots in time given a radial force F_x. The resultant perturbation in the bearing stiffness is illustrated in Fig. 2(c).

In the subsequent analysis, the rotation effect of Eq. (1) is applied to the $[K]_{bm}$ model developed by Lim and Singh [1,5] to give rise to a new time-varying formulation. For ball bearings, the elastic deformation $\delta_{Bs}(\psi_s(t))$ of the sth element is

$$\delta_{Bs}(\psi_s(t)) = \begin{cases} A(\psi_s(t)) - A_0, & \delta_{Bs} > 0 \\ 0, & \delta_{Bs} \leqslant 0 \end{cases}, \tag{2a}$$

$$A(\psi_s(t)) = \sqrt{\{A_0\cos(\alpha_0) + (\delta)_{rs}\}^2 + \{A_0\sin(\alpha_0) + (\delta)_{zs}\}^2}, \tag{2b}$$

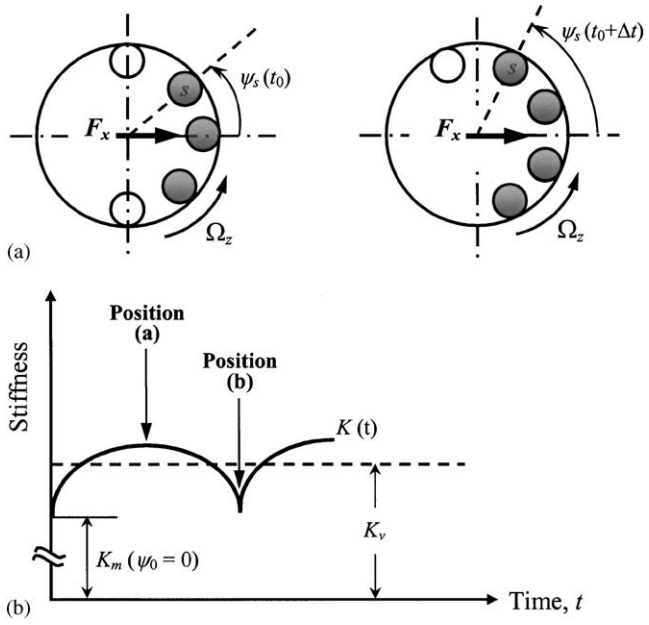

Fig. 2. Time-variation effect of the orbital motion on radially loaded rolling element bearing stiffness: (a) loaded elements (shaded circles) at time t_0; (b) loaded elements at time $t_0 + \Delta t$; (c) expected time variation in radial stiffness.

where A and A_0 are the loaded and unloaded relative distance between the inner a_i and outer a_o, raceway groove curvature centers. In Eq. (2a), $\delta_{Bs} \leqslant 0$ implies that the element is stress free. The net radial $(\delta)_{rs}$ and axial $(\delta)_{zs}$ displacements are given by

$$(\delta)_{rs} = \delta_{xm} \cos(\psi_s(t)) + \delta_{ym} \sin(\psi_s(t)) - r_L, \tag{3a}$$

$$(\delta)_{zs} = \delta_{zm} + r_d\{\beta_{xm} \sin(\psi_s(t)) - \beta_{ym} \cos(\psi_s(t))\}, \tag{3b}$$

where r_L is the bearing radial clearance, and δ_{im}, β_{wm} are the translational and angular displacements, respectively. Here, the subscript i can take on the bearing coordinate x, y or z, and w only refers to x or y. Note that Eq. (3) applies to roller type as well, and will be discussed later.

From the Hertzian theory, the load-deflection relation of a single element is given by

$$Q_s = K_n \delta_s^n, \tag{4}$$

where Q_s is the normal load, K_n is the Hertzian stiffness coefficient that is a function of materials and dimensions of element and raceways, and δ_s is given in Eq. (2a). The superscript n is the element load-deflection exponent that is exactly $\frac{3}{2}$ for ball type with elliptical contact. By performing a vector sum of all the non-zero element loads Q_s, i.e. $\delta_s > 0$, the resultant bearing loads and moments can be shown to be

$$\begin{Bmatrix} F_{bxm} \\ F_{bym} \\ F_{bzm} \\ M_{bxm} \\ M_{bym} \end{Bmatrix} = \sum_s^Z Q_s \begin{Bmatrix} \cos(\alpha_s)\cos(\psi_s(t)) \\ \cos(\alpha_s)\sin(\psi_s(t)) \\ \sin(\alpha_s) \\ r_d \sin(\alpha_s)\sin(\psi_s(t)) \\ -r_d \sin(\alpha_s)\cos(\psi_s(t)) \end{Bmatrix}, \tag{5}$$

where F_{bim}, M_{bwm}, $i = x, y, z$ and $w = x, y$, are the mean force and moment of the corresponding coordinate i or w, respectively, and α_s is the instantaneous contact angle of the sth element. Then by evaluating the partial derivatives of the bearing loads with respect to each bearing displacement term, a symmetric bearing stiffness matrix $[K(t)]_{bm}$, i.e., $k_{bij} = k_{bji}$, that is periodic in time can be formulated as

$$[K(t)]_{bm} = \begin{bmatrix} \partial F_{bim}/\partial \delta_{jm} & \partial F_{bim}/\partial \beta_{jm} \\ \partial M_{bim}/\partial \delta_{jm} & \partial M_{bim}/\partial \beta_{jm} \end{bmatrix}, \quad i, j = x, y, z. \tag{6}$$

The elements of the matrix for ball bearing are explicitly given in Appendix A.

For roller bearing, the elastic deformation $\delta_{Rs}(\psi_s(t), \zeta)$ of the sth element is a function of both $\psi_s(t)$ and the normalized length ζ that accounts for load distribution along the roller axis:

$$\delta_{Rs}(\psi_s(t), \zeta) = \begin{Bmatrix} V(\psi_s(t)) + \zeta L W(\psi_s(t)), & \delta_{Rs} > 0 \\ 0, & \delta_{Rs} \leqslant 0 \end{Bmatrix}, \quad -0.5 \leqslant \zeta \leqslant 0.5, \tag{7a}$$

$$V(\psi_s(t)) = (\delta)_{rs} \cos(\alpha_s) + (\delta)_{zs} \sin(\alpha_s) - r_c, \tag{7b}$$

$$W(\psi_s(t)) = -\beta_{xm} \sin(\psi_s(t)) + \beta_{ym} \cos(\psi_s(t)), \tag{7c}$$

where r_c is the crown drop. Again, applying the Hertzian contact stress principle and integrating along the roller contact line yields the load-deflection relation for the sth element:

$$Q_s = K_n \int_{\zeta_1}^{\zeta_2} \{V(\psi_s(t)) + \zeta LW(\psi_s(t))\}^n \, \mathrm{d}\zeta, \tag{8}$$

where n now is equal to $\frac{10}{9}$ assuming a rectangular contact area. The subset (ζ_1, ζ_2) in Eq. (8) is bounded by the following limits of integration given by

$$\zeta_1 = \begin{Bmatrix} \max[-V(\psi_s(t))/LW(\psi_s(t)), -0.5], & LW(\psi_s(t)) > 0 \\ -0.5, & LW(\psi_s(t)) \leqslant 0 \end{Bmatrix}, \tag{9a}$$

$$\zeta_2 = \begin{Bmatrix} 0.5, & LW(\psi_s(t)) \geqslant 0 \\ \min[-V(\psi_s(t))/LW(\psi_s(t)), 0.5], & LW(\psi_s(t)) < 0 \end{Bmatrix}. \tag{9b}$$

The resultant bearing loads can then be attained by doing a vector sum of all non-zero element loads Q_s:

$$\begin{Bmatrix} F_{bxm} \\ F_{bym} \\ F_{bzm} \\ M_{bxm} \\ M_{bym} \end{Bmatrix} = \sum_{s}^{Z} Q_s \begin{Bmatrix} \cos(\alpha_s)\cos(\psi_s(t)) \\ \cos(\alpha_s)\sin(\psi_s(t)) \\ \sin(\alpha_s) \\ (r_d \sin(\alpha_s) + e_s)\sin(\psi_s(t)) \\ -(r_d \sin(\alpha_s) + e_s)\cos(\psi_s(t)) \end{Bmatrix}, \tag{10a}$$

$$e_s = \frac{L \int_{\zeta_1}^{\zeta_2} \zeta \{V(\psi_s(t), \zeta) + \zeta LW(\psi_s(t), \zeta)\}^n \, \mathrm{d}\zeta}{\int_{\zeta_1}^{\zeta_2} \{V(\psi_s(t), \zeta) + \zeta LW(\psi_s(t), \zeta)\}^n \, \mathrm{d}\zeta}. \tag{10b}$$

From the load-displacement relations given above, the roller bearing stiffness matrix $[K(t)]_{bm}$ can be derived by evaluating the appropriate partial derivatives as shown in Eq. (6). The explicit expressions for the roller bearing stiffness terms are given in Appendix B.

For both ball and roller types, the instantaneous time-varying stiffness coefficients can be represented in a more general form as $K_{bij}(t) = K_{bij,v} + K_{bij,a}(t)$, $i,j =$ is $x, y, z, \theta_x, \theta_y, \theta_z$. In this form, $K_{bij,a}(t)$ is in fact the periodic component that fluctuates about the mean stiffness $K_{bij,v}$.

3. Parametric analysis

The bearing systems previously studied by Lim and Singh [1,5] are re-analyzed here to determine the effect of orbital motion Ω_z. To demonstrate the nature of time-variation, the stiffness coefficients are computed as a function of the normalized orbital position angle given by ψ/ψ_T where $\psi_T = 2\pi/Z$ radians is the element-to-element angular distance. Figs. 3 and 4 plot the dominant K_{bij} terms for a radially loaded angular contact ball type ($\alpha_0 > 0^\circ$) and a straight roller bearing ($\alpha \approx 0^\circ$), respectively. The results clearly show the periodic nature of the stiffness coefficients with the fundamental time period given by ψ_T/Ω_z. For these same cases, the calculations by Lim and Singh only give a single value for each K_{bij}. Most of the terms in Fig. 3

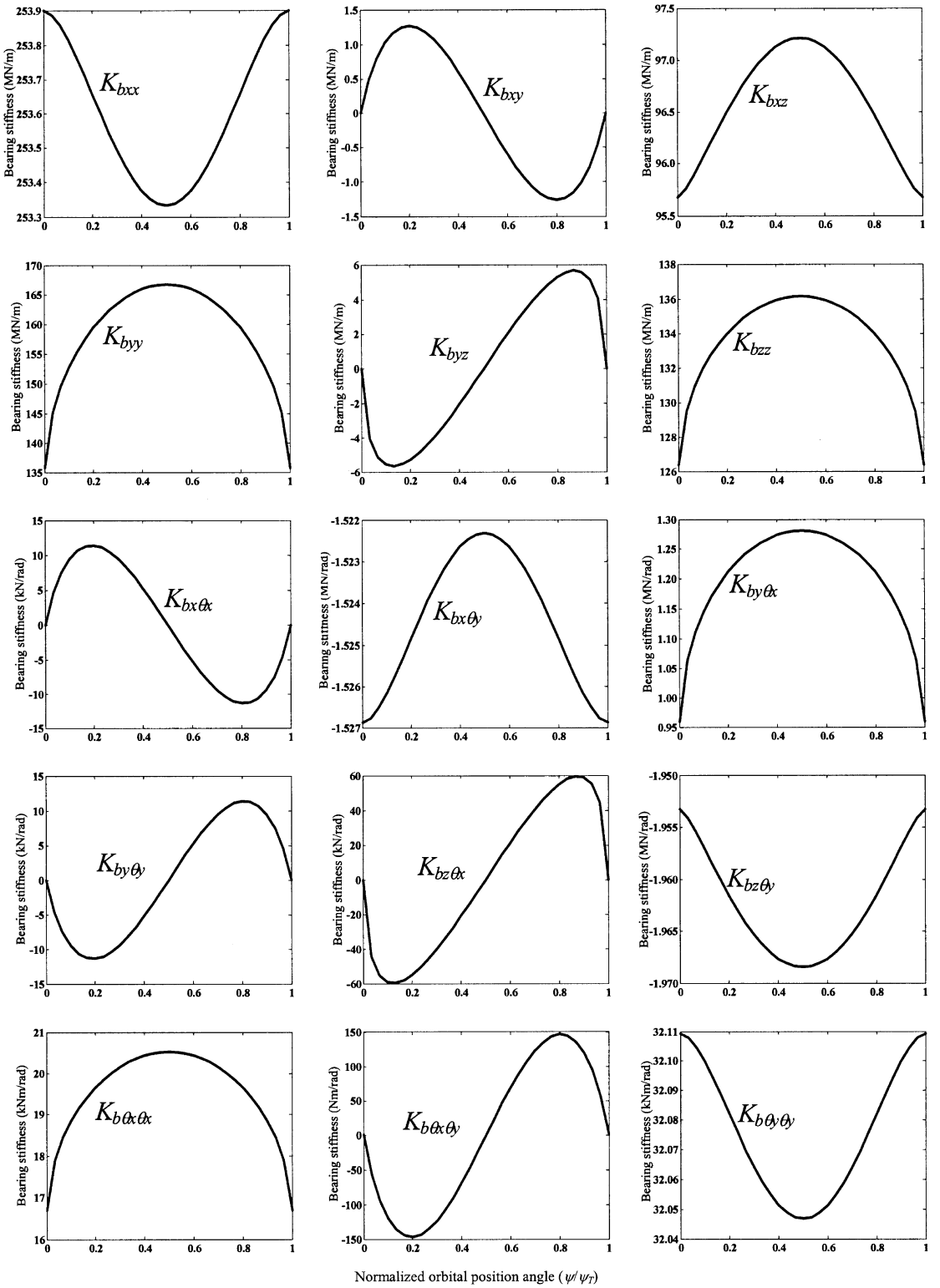
Bearing stiffness (MN/m)
K_{bxx}
Bearing stiffness (MN/m)
K_{bxy}
Bearing stiffness (MN/m)
K_{bxz}
Bearing stiffness (MN/m)
K_{byy}
Bearing stiffness (MN/m)
K_{byz}
Bearing stiffness (MN/m)
K_{bzz}
Bearing stiffness (kN/rad)
$K_{bx\theta x}$
Bearing stiffness (MN/rad)
$K_{bx\theta y}$
Bearing stiffness (MN/rad)
$K_{by\theta x}$
Bearing stiffness (kN/rad)
$K_{by\theta y}$
Bearing stiffness (kN/rad)
$K_{bz\theta x}$
Bearing stiffness (MN/rad)
$K_{bz\theta y}$
Bearing stiffness (kNm/rad)
$K_{b\theta x\theta x}$
Bearing stiffness (Nm/rad)
$K_{b\theta x\theta y}$
Bearing stiffness (kNm/rad)
$K_{b\theta y\theta y}$
Normalized orbital position angle (ψ/ψ_T)

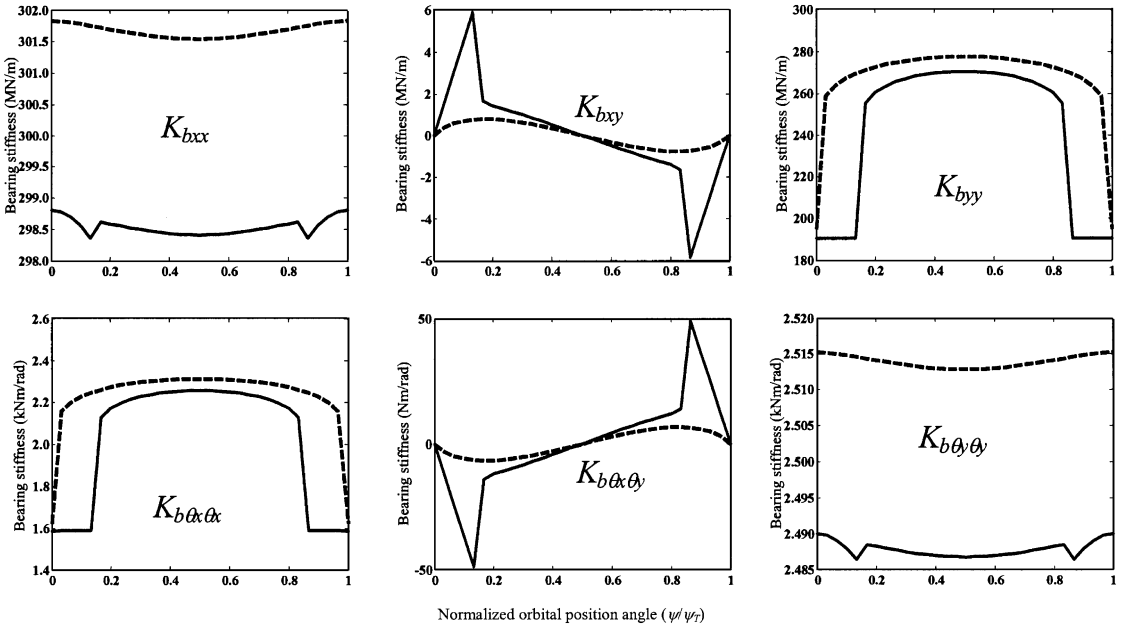

Fig. 4. Variation in the dominant stiffness coefficients of a radially loaded roller bearing for $\delta_{xm} = 0.025\,\text{mm}$, $r_d = 21.25\,\text{mm}$, $\alpha_0 = 0^\circ$, $R_L = 10\,\text{mm}$, $r_b = 3\,\text{mm}$, $r_L = 0.00175\,\text{mm}$, $Z = 12$, $K_n = 3 \times 10^8\,\text{N/m}^n$, and $n = 10/9$ (——, $r_L = 0.00175\,\text{mm}$; - - - - -, $r_L = 0$).

(ball type) appear nearly sinusoidal except K_{bzz}, $K_{by\theta x}$ and $K_{b\theta x\theta x}$ that vary like a rectified sine wave. The discontinuity observed in Fig. 4 (roller type) is essentially due to the variation in the number of loaded rolling elements within one element-to-element cycle, and is more acute when radial clearance is greater.

The ratio of the peak-to-peak to root-mean-square (PPRMS) parameter is proposed to assess the depth of variation of the bearing stiffness coefficient. For the same two ball and roller cases, their PPRMS ratios are given in Figs. 5 and 6, respectively, as a function of the unloaded contact angle α_0. Results show, for both cases, the largest PPRMS levels are observed in the translational stiffness coefficients K_{bxy} and K_{byz}, the translational-rotational stiffness coefficients $K_{bz\theta x}$, $K_{bx\theta x}$, and $K_{by\theta y}$, and the rotational stiffness coefficient $K_{b\theta x\theta y}$. Hence, these terms are expected to have the most significant contributions to the difference between a linear time-invariant and a time-varying vibration response.

4. Geared rotor system

As an example, a lumped parameter dynamic model of the bearing supported gear pair system shown in Fig. 7 is examined to determine the extent of the effect of time-variation in bearing

Fig. 3. Variation in the dominant stiffness coefficients of a radially loaded ball bearing for $\delta_{xm} = 0.025\,\text{mm}$, $r_d = 19.65\,\text{mm}$, $A_0 = 0.05\,\text{mm}$, $\alpha_0 = 30^\circ$, $r_b = 3\,\text{mm}$, $r_L = 0.00005\,\text{mm}$, $Z = 12$, $K_n = 1.45 \times 10^{10}\,\text{N/m}^n$, and $n = 3/2$.

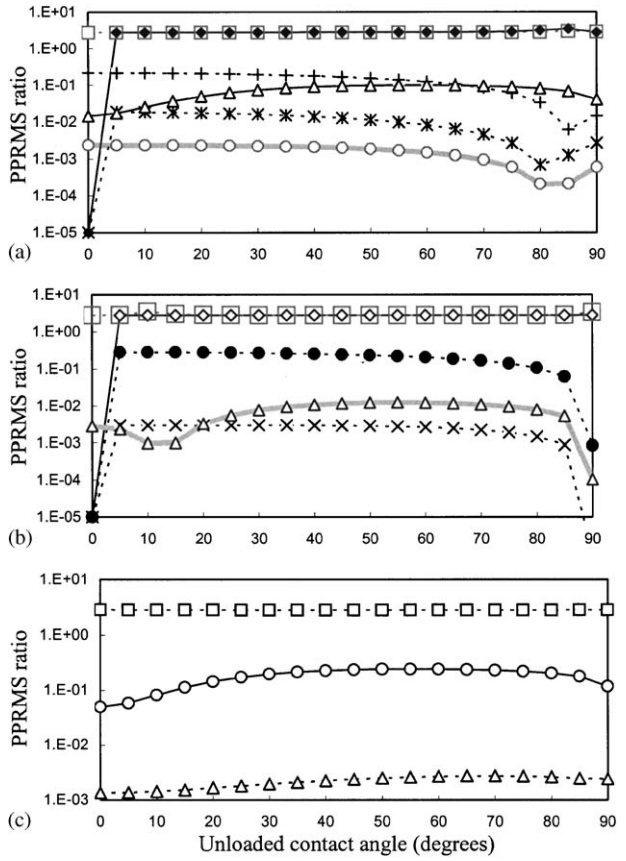

Fig. 5. Effect of α_0 on the PPRMS of dominant stiffness coefficients of the radially loaded ball bearing results of Fig. 3. (a) —○—, K_{bxx}; - - -□- - -, K_{bxy}; – – ∗ – –, K_{bxz}; – – + – –, K_{byy}; —◆—, K_{byz}; —△—, K_{bzz}; (b) —◇—, $K_{bx\theta x}$, $K_{by\theta y}$; -- ×--, $K_{bx\theta y}$; – – ● – –, $K_{by\theta x}$; ▬ ▭ ▬, $K_{bz\theta x}$; ▬△▬, $K_{bz\theta y}$; (c) —○—, $K_{b\theta x\theta x}$; – – □ – –, $K_{b\theta x\theta y}$; – – △ – –, $K_{b\theta y\theta y}$.

stiffness on vibration response. The linear time-varying (LTV) formulation can generally be represented as

$$[M]\{\ddot{q}(t)\} + [C(t)]\{\dot{q}(t)\} + [K(t)]\{q(t)\} = \{f(t)\}, \tag{11}$$

where $\{q(t)\}$ is $\{x_p \;\; y_p \;\; z_p \;\; \theta_{xp} \;\; \theta_{yp} \;\; \theta_{zp} \;\; x_g \;\; y_g \;\; z_g \;\; \theta_{xg} \;\; \theta_{yg} \;\; \theta_{zg}\}^{\mathrm{T}}$. The mass matrix $[M]$ can be written as

$$[M] = \mathrm{diag}\{\{m\}_p^{\mathrm{T}}\{I\}_p^{\mathrm{T}} | \{m\}_g^{\mathrm{T}}\{I\}_g^{\mathrm{T}}\}, \tag{12}$$

Here, m stands for mass, I represents mass moment of inertia, subscripts p, g refer to the pinion and gear, and superscript T is the transpose operation. The system stiffness matrix $[K(t)]$ is explicitly given in Appendix C, while the damping matrix is assumed $[C(t)] = \beta[K(t)]$ where β is the proportionality constant. The applied load vector $\{f(t)\}$ due to the transmission error

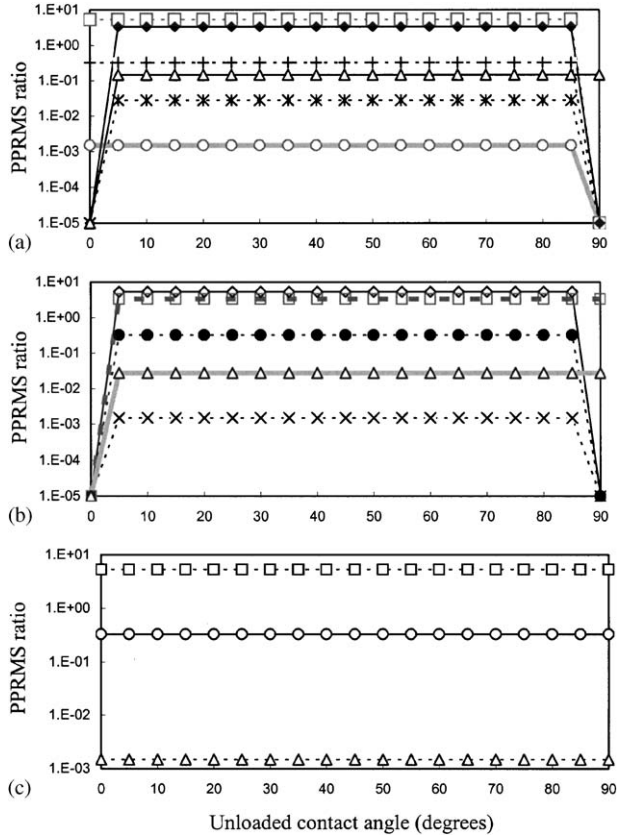

Fig. 6. Effect of α_0 on the PPRMS of dominant stiffness coefficients of the radially loaded roller bearing results of Fig. 4. (a) —○—, K_{bxx}; - - -□- - -, K_{bxy}; – – ∗ – –, K_{bxz}; – – + – –, K_{byy}; —◆—, K_{byz}; —△—, K_{bzz}; (b) —◇—, $K_{bx\theta x}$, $K_{by\theta y}$; - -×- -, $K_{bx\theta y}$; – – ● – –, $K_{by\theta x}$; ▬ ▭ ▬, $K_{bz\theta x}$; ▬△▬, $K_{bz\theta y}$; (c) —○—, $K_{b\theta x\theta x}$; – – □ – –, $K_{b\theta x\theta y}$; – – △ – –, $K_{b\theta y\theta y}$.

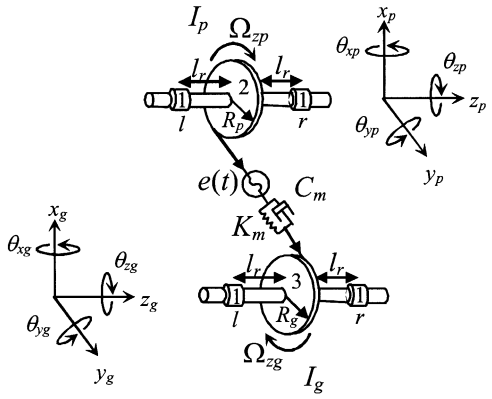

Fig. 7. Geared rotor system model with transmission error $e(t)$ as the primary excitation function. Rolling element bearing, 1; pinion, 2; gear, 3; $m_g = m_p = 0.5\,\text{kg}$; $I_g = I_p = 3.0 \times 10^{-4}\,\text{kg m}^{-2}$; $R_g = R_p = 34.6\,\text{mm}$; $K_m = 1.0 \times 10^8\,\text{N/m}$; $l_r = 25\,\text{mm}$; pressure angle = 20°; number of teeth = 28.

excitation $e(t)$ is

$$\{f(t)\} = \begin{Bmatrix} 0 \\ -K_m e(t) - C_m \dot{e}(t) \\ 0 \\ 0 \\ 0 \\ K_m R_p e(t) + C_m R_p \dot{e}(t) \\ 0 \\ K_m e(t) + C_m \dot{e}(t) \\ 0 \\ 0 \\ 0 \\ K_m R_g e(t) + C_m R_g \dot{e}(t) \end{Bmatrix}, \tag{13}$$

where K_m is the gear mesh stiffness and C_m is the mesh damping coefficient. The time-varying governing equation (11) can be solved for the steady-state vibrations using the Runge–Kutta time-integration scheme. For time-invariant cases where $[K]$ is constant, the steady-state response vector in the frequency domain is $\{\bar{q}(\omega)\} = (-\omega^2[M] + i\omega[C] + [K])^{-1}\{\bar{f}(\omega)\}$. Two time-invariant cases are analyzed here. One is the linear time-invariant (LTI) case similar to the analysis by Lim and Singh, which consists of constant bearing stiffnesses based on fixed element position. The other is the mean linear time-varying (MLTV) case formulated from averaging the bearing stiffness values over one element-to-element angular distance.

Using the three different models described above, the vibration response functions of the geared rotor system due to transmission error excitation are shown in Figs. 8 and 9 for angular contact ball bearing and straight roller bearing applications, respectively. For each case, the pinion and gear translational and rotational response are computed. The translational motion is parallel to the gear mesh line-of-action that is along the pressure angle direction. From the response computed, it is quite clear that the MLTV predictions give nearly the same results as the true linear time-varying (LTV) model. On the other hand, the LTI model tends to underestimate the resonance frequency even though the peak amplitude is not too far off from both the LTV and MLTV results. This is evident from Table 1 that lists the natural frequency deviations of both LTI and MLTV modes, and also from the locations of peak responses seen in Figs. 8 and 9. Note that the pinion and gear behaviors are nearly identical due to the symmetry of the system defined. From these results, we can conclude that the time-variation effect is moderate.

However, the models do show that adopting the averaged bearing stiffness formulation is sufficient, which a slight improvement over the earlier quasi-static, fixed element position, bearing model proposed by Lim and Singh.

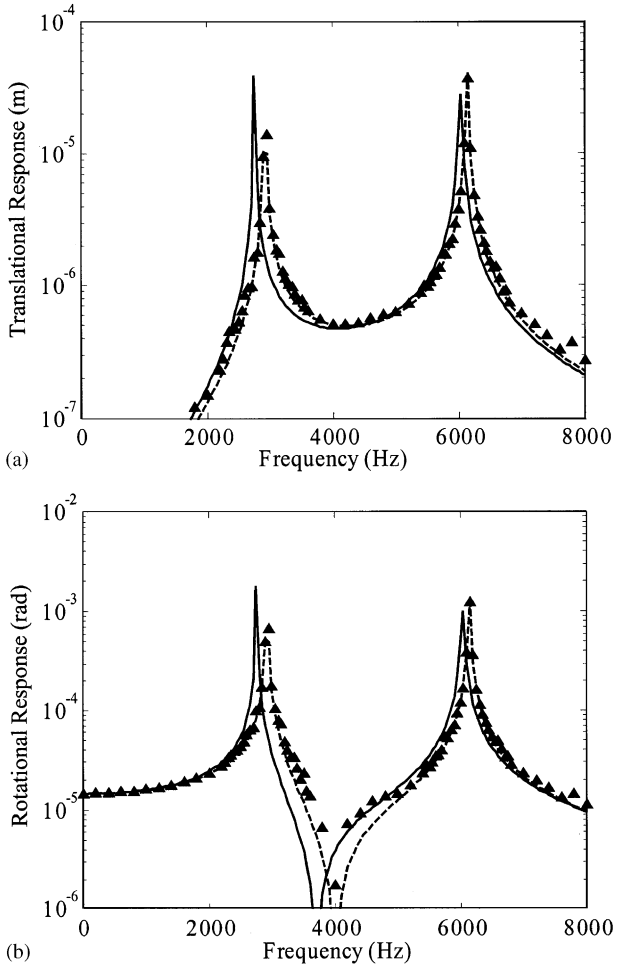

Fig. 8. Vibration response of the geared rotor system supported by angular contact ball bearing under radial preload (see Fig. 3 for bearing parameter) due to transmission error excitation: (a) pinion/gear translation motion along the y-direction; (b) pinion/gear rotational motion about the z-axis. (▲, LTV; - - - - -, MLTV; ——, LTI.)

5. Summary

A new time-varying rolling element bearing stiffness formulation is proposed by extending an earlier quasi-static, linear time-invariant theory. The formulation takes into the account of the effect of shaft rotational speed that causes the orbital motion of the rolling elements of the bearings, which in turn produces time-varying, periodic load and stiffness patterns. The nature of the time-varying stiffness coefficients is also studied generally by transforming the dependence on shaft speed and time into a function of normalized orbital position angle. The proposed time-varying theory provides a basis for an improved time-averaged bearing stiffness model that yield comparable predictions for a gear pair example to the direct numerical integration results. The new model is a slight improvement over the earlier quasi-static, fixed element position, bearing stiffness formulation.

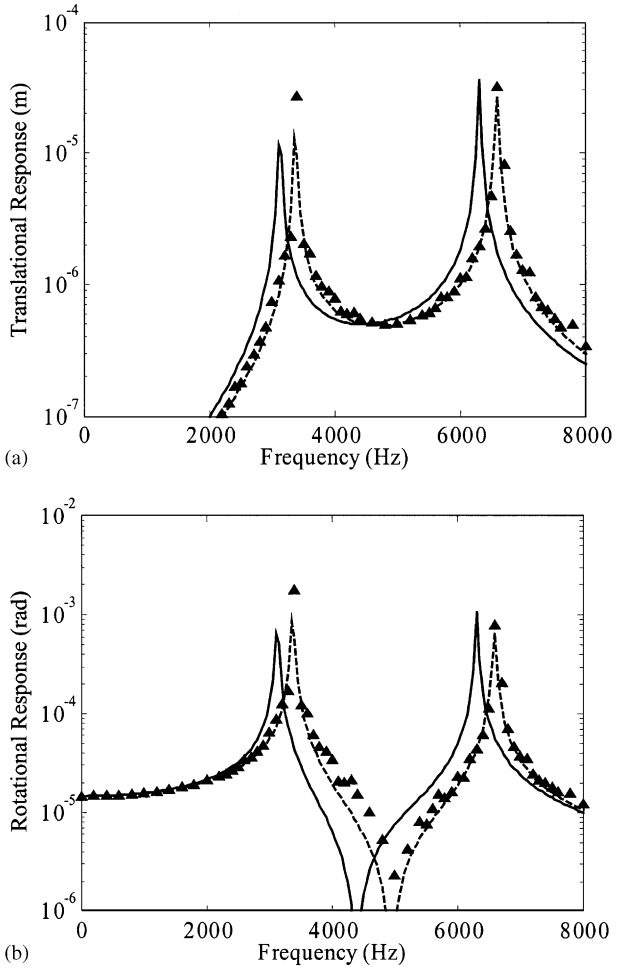

Fig. 9. Vibration response of the geared rotor system supported by straight roller bearing under radial preload (see Fig. 4 for bearing parameter) due to transmission error excitation: (a) pinion/gear translation motion along the y-direction; (b) pinion/gear rotational motion about the z-axis. (▲, LTV; -----, MLTV; ——, LTI.)

Appendix A. Expression of the ball bearing stiffness coefficients

$$K_{bxx} = K_n \sum_{s}^{z} \frac{(A_s - A_0)^n \cos^2(\psi_s(t)) \left\{ \frac{nA_s(\delta^*)_{rs}^2}{A_s - A_0} + A_s^2 - (\delta^*)_{rs}^2 \right\}}{A_s^3},$$

$$K_{bxy} = K_n \sum_{s}^{z} \frac{(A_s - A_0)^n \sin(\psi_s(t)) \cos(\psi_s(t)) \left\{ \frac{nA_s(\delta^*)_{rs}^2}{A_s - A_0} + A_s^2 - (\delta^*)_{rs}^2 \right\}}{A_s^3},$$

Table 1
Natural frequency (Hz) comparisons of flexible geared rotor system modes

Mode	f_{LTI}	f_{MLTV}	Δ (%)
Angular contact ball bearing			
1,2	1444	1581	8.7
3	2761	2929	5.7
4	3709	4006	7.4
5,6	4141	4474	7.4
7,8	5072	5069	0.1
9	6040	6150	1.7
10,11	6553	6574	0.3
Straight roller bearing			
1	3128	3376	7.3
2	4391	4949	11.3
3,4	5653	5651	~ 0.0
5	6313	6591	4.2

$\Delta(\%) = |(f_{\mathrm{MLTV}} - f_{\mathrm{LTI}})/f_{\mathrm{MLTV}}| \times 100.$

$$K_{bxz} = K_n \sum_s^z \frac{(A_s - A_0)^n (\delta^*)_{rs} (\delta^*)_{zs} \cos(\psi_s(t)) \left\{ \frac{nA_s}{A_s - A_0} - 1 \right\}}{A_S^3},$$

$$K_{bx\theta x} = K_n \sum_s^z \frac{r_d (A_s - A_0)^n (\delta^*)_{rs} (\delta^*)_{zs} \sin(\psi_s(t)) \cos(\psi_s(t)) \left\{ \frac{nA_s}{A_s - A_0} - 1 \right\}}{A_s^3},$$

$$K_{bx\theta y} = K_n \sum_s^z \frac{r_d (A_s - A_0)^n (\delta^*)_{rs} (\delta^*)_{zs} \cos^2(\psi_s(t)) \left\{ 1 - \frac{nA_s}{A_s - A_0} \right\}}{A_s^3},$$

$$K_{byy} = K_n \sum_s^z \frac{(A_s - A_0)^n \sin^2(\psi_s(t)) \left\{ \frac{nA_s (\delta^*)_{rs}^2}{A_s - A_0} + A_s^2 - (\delta^*)_{rs}^2 \right\}}{A_s^3},$$

$$K_{byz} = K_n \sum_s^z \frac{(A_s - A_0)^n (\delta^*)_{rs} (\delta^*)_{zs} \sin(\psi_s(t)) \left\{ \frac{nA_s}{A_s - A_0} - 1 \right\}}{A_s^3},$$

$$K_{by\theta x} = K_n \sum_s^z \frac{r_d (A_s - A_0)^n (\delta^*)_{rs} (\delta^*)_{zs} \sin^2(\psi_s(t)) \left\{ \frac{nA_s}{A_s - A_0} - 1 \right\}}{A_s^3},$$

$$K_{by\theta y} = K_n \sum_s^z \frac{r_d(A_s - A_0)^n(\delta^*)_{rs}(\delta^*)_{zs} \sin(\psi_s(t)) \cos(\psi_s(t))\left\{1 - \frac{nA_s}{A_s - A_0}\right\}}{A_s^3},$$

$$K_{bzz} = K_n \sum_s^z \frac{(A_s - A_0)^n \left\{\frac{nA_s(\delta^*)_{zs}^2}{A_s - A_0} + A_s^2 - (\delta^*)_{zs}^2\right\}}{A_s^3},$$

$$K_{bz\theta x} = K_n \sum_s^z \frac{r_d(A_s - A_0)^n \sin(\psi_s(t))\left\{\frac{nA_s(\delta^*)_{zs}^2}{A_s - A_0} + A_s^2 - (\delta^*)_{zs}^2\right\}}{A_s^3},$$

$$K_{bz\theta y} = K_n \sum_s^z \frac{r_d(A_s - A_0)^n \cos(\psi_s(t))\left\{(\delta^*)_{zs}^2 - \frac{nA_s(\delta^*)_{zs}^2}{A_s - A_0} + A_s^2\right\}}{A_s^3},$$

$$K_{b\theta x\theta x} = K_n \sum_s^z \frac{r_d^2(A_s - A_0)^n \sin^2(\psi_s(t))\left\{\frac{nA_s(\delta^*)_{zs}^2}{A_s - A_0} + A_s^2 - (\delta^*)_{zs}^2\right\}}{A_s^3},$$

$$K_{b\theta x\theta y} = K_n \sum_s^z \frac{r_d^2(A_s - A_0)^n \sin(\psi_s(t)) \cos(\psi_s(t))\left\{(\delta^*)_{zs}^2 - \frac{nA_s(\delta^*)_{zs}^2}{A_s - A_0} - A_s^2\right\}}{A_s^3},$$

$$K_{b\theta y\theta y} = K_n \sum_s^z \frac{r_d^2(A_s - A_0)^n \cos^2(\psi_s(t))\left\{\frac{nA_s(\delta^*)_{zs}^2}{A_s - A_0} + A_s^2 - (\delta^*)_{zs}^2\right\}}{A_s^3},$$

$$K_{bi\theta z} = K_{b\theta i\theta z} = 0, \quad i = x, y, z.$$

Appendix B. Expressions of the roller bearing stiffness coefficients

$$K_{bxx} = nK_n \cos^2(\alpha_0) \sum_s^z I_0 \cos^2(\psi_s(t)),$$

$$K_{bxy} = nK_n \cos^2(\alpha_0) \sum_s^z I_0 \cos(\psi_s(t)) \sin(\psi_s(t)),$$

$$K_{bxz} = nK_n \cos(\alpha_0) \sin(\alpha_0) \sum_s^z I_0 \cos(\psi_s(t)),$$

$$K_{bx\theta x} = nK_n \cos(\alpha_0) \sum_s^z (I_0 r_d \sin(\alpha_0) - I_1) \cos(\psi_s(t)) \sin(\psi_s(t)),$$

$$K_{bx\theta y} = nK_n \cos(\alpha_0) \sum_s^z (I_1 - I_0 r_d \sin(\alpha_0)) \cos^2(\psi_s(t)),$$

$$K_{byy} = nK_n \cos^2(\alpha_0) \sum_s^z I_0 \sin^2(\psi_s(t)),$$

$$K_{byz} = nK_n \cos(\alpha_0) \sin(\alpha_0) \sum_s^z I_0 \sin(\psi_s(t)),$$

$$K_{by\theta x} = nK_n \cos(\alpha_0) \sum_s^z (I_0 r_d \sin(\alpha_0) - I_1) \sin^2(\psi_s(t)),$$

$$K_{by\theta y} = -K_{bx\theta x},$$

$$K_{bzz} = nK_n \sin^2(\alpha_0) \sum_s^z I_0,$$

$$K_{bz\theta x} = nK_n \sin(\alpha_0) \sum_s^z (I_0 r_d \sin(\alpha_0) - I_1) \sin(\psi_s(t)),$$

$$K_{bz\theta y} = nK_n \sin(\alpha_0) \sum_s^z (I_1 - I_0 r_d \sin(\alpha_0)) \cos(\psi_s(t)),$$

$$K_{b\theta x\theta x} = nK_n \sum_s^z (I_0 r_d^2 \sin^2(\alpha_0) - 2I_1 r_d \sin(\alpha_0) + I_2) \sin^2(\psi_s(t)),$$

$$K_{b\theta x\theta y} = nK_n \sum_s^z (2I_1 r_d \sin(\alpha_0) - I_0 r_d^2 \sin^2(\alpha_0) - I_2) \sin(\psi_s(t)) \cos(\psi_s(t)),$$

$$K_{b\theta y\theta y} = nK_n \sum_s^z (I_0 r_d^2 \sin^2(\alpha_0) - 2I_1 r_d \sin(\alpha_0) + I_2) \cos^2(\psi_s(t)),$$

$$K_{bi\theta z} = K_{b\theta i\theta z} = 0, \quad i = x, y, z,$$

where I_u and $T(u, \zeta)$ are given by

$$I_u = T(u, \zeta_2) - T(u, \zeta_1), \quad u = 0, 1 \text{ or } 2,$$

$$T(u, \zeta) = \begin{cases} \frac{(V+\zeta LW)^n}{nW} \left[(L\zeta)^u - \frac{u(L\zeta)^{u-1}(V+\zeta LW)^1}{(n+1)W} + \frac{u(u-1)(V+\zeta LW)^2}{(n+1)(n+2)W^2} \right], & W \neq 0 \\ \frac{(L\zeta)^{u+1} V^{n-1}}{u+1}, & W = 0 \end{cases}.$$

Appendix C. Expressions of the system stiffness coefficients for Eq. (11)

$$
[K(t)] = \begin{bmatrix}
[K]_{11} & [K]_{12} & [K]_{13} & [K]_{14} & [K]_{15} & [K]_{16} & 0 & 0 & 0 & 0 & 0 & 0 \\
[K]_{21} & [K]_{22} & [K]_{23} & [K]_{24} & [K]_{25} & [K]_{26} & 0 & -K_m & 0 & 0 & 0 & -K_m R_g \\
[K]_{31} & [K]_{32} & [K]_{33} & [K]_{34} & [K]_{35} & [K]_{36} & 0 & 0 & 0 & 0 & 0 & 0 \\
[K]_{41} & [K]_{42} & [K]_{43} & [K]_{44} & [K]_{45} & [K]_{46} & 0 & 0 & 0 & 0 & 0 & 0 \\
[K]_{51} & [K]_{52} & [K]_{53} & [K]_{54} & [K]_{55} & [K]_{56} & 0 & 0 & 0 & 0 & 0 & 0 \\
[K]_{61} & [K]_{62} & [K]_{63} & [K]_{64} & [K]_{65} & [K]_{66} & 0 & K_m R_p & 0 & 0 & 0 & K_m R_p R_g \\
0 & 0 & 0 & 0 & 0 & 0 & [K]_{77} & [K]_{78} & [K]_{79} & [K]_{7,10} & [K]_{7,11} & [K]_{7,12} \\
0 & -K_m & 0 & 0 & 0 & K_m R_p & [K]_{87} & [K]_{88} & [K]_{89} & [K]_{8,10} & [K]_{8,11} & [K]_{8,12} \\
0 & 0 & 0 & 0 & 0 & 0 & [K]_{97} & [K]_{98} & [K]_{99} & [K]_{9,10} & [K]_{9,11} & [K]_{9,12} \\
0 & 0 & 0 & 0 & 0 & 0 & [K]_{10,7} & [K]_{10,8} & [K]_{10,9} & [K]_{10,10} & [K]_{10,11} & [K]_{10,12} \\
0 & 0 & 0 & 0 & 0 & 0 & [K]_{11,7} & [K]_{11,8} & [K]_{11,9} & [K]_{11,10} & [K]_{11,11} & [K]_{11,12} \\
0 & -K_m R_g & 0 & 0 & 0 & K_m R_p R_g & [K]_{12,7} & [K]_{12,8} & [K]_{12,9} & [K]_{12,10} & [K]_{12,11} & [K]_{12,12}
\end{bmatrix}
$$

$$
\begin{aligned}
&[K]_{11} = [K_{bxx}]_{lp} + [K_{bxx}]_{rp}, \quad [K]_{12} = [K_{bxy}]_{lp} + [K_{bxy}]_{rp}, \quad [K]_{13} = [K_{bxz}]_{lp} + [K_{bxz}]_{rp},\\
&[K]_{14} = [K_{bx\theta x}]_{lp} + [K_{bx\theta x}]_{rp} + \{[K_{bxy}]_{lp} - [K_{bxy}]_{rp}\} l_r,\\
&[K]_{15} = [K_{bx\theta y}]_{lp} + [K_{bx\theta y}]_{rp} + \{[K_{bxx}]_{rp} - [K_{bxx}]_{lp}\} l_r, \quad [K]_{16} = [K_{bx\theta z}]_{lp} + [K_{bx\theta z}]_{rp},\\
&[K]_{22} = [K_{byy}]_{lp} + [K_{byy}]_{rp} + K_m, \quad [K]_{23} = [K_{byz}]_{lp} + [K_{byz}]_{rp},\\
&[K]_{24} = [K_{by\theta x}]_{lp} + [K_{by\theta x}]_{rp} + \{[K_{byy}]_{lp} - [K_{byy}]_{rp}\} l_r,\\
&[K]_{25} = [K_{by\theta y}]_{lp} + [K_{by\theta y}]_{rp} + \{[K_{byx}]_{rp} - [K_{byx}]_{lp}\} l_r, \quad [K]_{26} = [K_{by\theta z}]_{lp} + [K_{by\theta z}]_{rp} - K_m R_p,\\
&[K]_{33} = [K_{bzz}]_{lp} + [K_{bzz}]_{rp}, \quad [K]_{34} = [K_{bz\theta x}]_{lp} + [K_{bz\theta x}]_{rp} + \{[K_{bzy}]_{lp} - [K_{bzy}]_{rp}\} l_r,\\
&[K]_{35} = [K_{bz\theta y}]_{lp} + [K_{bz\theta y}]_{rp} + \{[K_{bzx}]_{rp} - [K_{bzx}]_{lp}\} l_r, \quad [K]_{36} = [K_{bz\theta z}]_{lp} + [K_{bz\theta z}]_{rp},\\
&[K]_{44} = [K_{b\theta x\theta x}]_{lp} + [K_{b\theta x\theta x}]_{rp} + \{[K_{byy}]_{lp} + [K_{byy}]_{rp}\} l_r^2 + \{[K_{b\theta xy}]_{lp} + [K_{b\theta xy}]_{rp}\} l_r,\\
&[K]_{45} = [K_{b\theta x\theta y}]_{lp} + [K_{b\theta x\theta y}]_{rp} + \{[K_{b\theta xx}]_{rp} + [K_{b\theta xx}]_{lp}\} l_r, \quad [K]_{46} = [K_{b\theta x\theta z}]_{lp} + [K_{b\theta x\theta z}]_{rp},\\
&[K]_{55} = [K_{b\theta y\theta y}]_{lp} + [K_{b\theta y\theta y}]_{rp} + \{[K_{bxx}]_{lp} + [K_{bxx}]_{rp}\} l_r^2 + \{[K_{b\theta yx}]_{rp} + [K_{b\theta yx}]_{lp}\} l_r,\\
&[K]_{56} = [K_{b\theta y\theta z}]_{lp} + [K_{b\theta y\theta z}]_{rp}, \quad [K]_{66} = [K_{b\theta z\theta z}]_{lp} + [K_{b\theta z\theta z}]_{rp} + K_m R_p^2,\\
&[K]_{77} = [K_{bxx}]_{\mathrm{lg}} + [K_{bxx}]_{rg}, \quad [K]_{78} = [K_{bxy}]_{\mathrm{lg}} + [K_{bxy}]_{rg},\\
&[K]_{79} = [K_{bxz}]_{\mathrm{lg}} + [K_{bxz}]_{rg}, \quad [K]_{7,10} = [K_{bx\theta x}]_{\mathrm{lg}} + [K_{bx\theta x}]_{rg} + \{[K_{bxy}]_{\mathrm{lg}} - [K_{bxy}]_{rg}\} l_r,\\
&[K]_{7,11} = [K_{bx\theta y}]_{\mathrm{lg}} + [K_{bx\theta y}]_{rg} + \{[K_{bxx}]_{rg} - [K_{bxx}]_{\mathrm{lg}}\} l_r, \quad [K]_{7,12} = [K_{bx\theta z}]_{\mathrm{lg}} + [K_{bx\theta z}]_{rg},\\
&[K]_{88} = [K_{byy}]_{\mathrm{lg}} + [K_{byy}]_{rg} + K_m, \quad [K]_{89} = [K_{byz}]_{\mathrm{lg}} + [K_{byz}]_{rg},
\end{aligned}
$$

$$[K]_{8,10} = [K_{by\theta x}]_{lg} + [K_{by\theta x}]_{rg} + \{[K_{byy}]_{lg} - [K_{byy}]_{rg}\}l_r,$$
$$[K]_{8,11} = [K_{by\theta y}]_{lg} + [K_{by\theta y}]_{rg} + \{[K_{byx}]_{rg} - [K_{byx}]_{lg}\}l_r,$$
$$[K]_{8,12} = [K_{by\theta z}]_{lg} + [K_{by\theta z}]_{rg} + K_m R_g,$$
$$[K]_{99} = [K_{bzz}]_{lg} + [K_{bzz}]_{rg}, \quad [K]_{9,10} = [K_{bz\theta x}]_{lg} + [K_{bz\theta x}]_{rg} + \{[K_{bzy}]_{lg} - [K_{bzy}]_{rg}\}l_r,$$
$$[K]_{9,11} = [K_{bz\theta y}]_{lg} + [K_{bz\theta y}]_{rg} + \{[K_{bzx}]_{rg} - [K_{bzx}]_{lg}\}l_r, \quad [K]_{9,12} = [K_{bz\theta z}]_{lg} + [K_{bz\theta z}]_{rg},$$
$$[K]_{10,10} = [K_{b\theta x\theta x}]_{lg} + [K_{b\theta x\theta x}]_{rg} + \{[K_{byy}]_{lg} + [K_{byy}]_{rg}\}l_r^2 + \{[K_{b\theta xy}]_{lg} + [K_{b\theta xy}]_{rg}\}l_r,$$
$$[K]_{10,11} = [K_{b\theta x\theta y}]_{lg} + [K_{b\theta x\theta y}]_{rg} + \{[K_{b\theta xx}]_{rg} + [K_{b\theta xx}]_{lg}\}l_r, \quad [K]_{10,12} = [K_{b\theta x\theta z}]_{lg} + [K_{b\theta x\theta z}]_{rg},$$
$$[K]_{11,11} = [K_{b\theta y\theta y}]_{lg} + [K_{b\theta y\theta y}]_{rg} + \{[K_{bxx}]_{lg} + [K_{bxx}]_{rg}\}l_r^2 + \{[K_{b\theta yx}]_{rg} + [K_{b\theta yx}]_{lg}\}l_r,$$
$$[K]_{11,12} = [K_{b\theta y\theta z}]_{lg} + [K_{b\theta y\theta z}]_{rg}, \quad [K]_{12,12} = [K_{b\theta z\theta z}]_{lg} + [K_{b\theta z\theta z}]_{rg} + K_m R_g^2,$$

where subscripts l, r, p and g refer to left bearing, right bearing, pinion and gear, respectively. Also, R_p and R_g are the pinion and gear pitch radii, l_r is the distance from pinion/gear to the bearing support location, and K_m is the gear mesh stiffness.

References

[1] T.C. Lim, R. Singh, Vibration transmission through rolling element bearings, part I: bearing stiffness formulation, *Journal of Sound and Vibration* 139 (2) (1990) 179–199.

[2] T.C. Lim, R. Singh, Vibration transmission through rolling element bearings, part II: system studies, *Journal of Sound and Vibration* 139 (2) (1990) 201–225.

[3] T.C. Lim, R. Singh, Vibration transmission through rolling element bearings, part III: geared rotor system studies, *Journal of Sound and Vibration* 151 (1) (1991) 31–54.

[4] T.C. Lim, R. Singh, Vibration transmission through rolling element bearings, part IV: statistical energy analysis, *Journal of Sound and Vibration* 153 (1) (1992) 37–50.

[5] T.C. Lim, R. Singh, Vibration transmission through rolling element bearings, part V: effect of distributed contact load on roller bearing stiffness matrix, *Journal of Sound and Vibration* 169 (4) (1994) 547–553.

[6] A.B. Jones, A general theory for elastically constrained ball and radial roller bearings under arbitrary load and speed conditions, *Journal of Basic Engineering* 82 (1960) 309–320.

[7] T.A. Harris, *Rolling Bearing Analysis*, Wiley, New York, 1984.

[8] A. Palmgren, *Ball and Roller Bearing Engineering*, Burbank, Philadelphia, 1959.

[9] M.F. White, Rolling element bearing vibration transfer characteristics: effect of stiffness, *Journal of Applied Mechanics* 46 (1979) 677–684.

[10] M.D. Rajab, Modeling of the Transmissibility Through Rolling Element Bearing under Radial and Moment Loads, PhD Dissertation, The Ohio State University, 1982.

[11] W.B. Young, Dynamics Modeling and Experimental Measurement of a Gear Shaft and Housing System, MS Thesis, The Ohio State University, 1988.

[12] L. Houpert, A uniform analytical approach for ball and roller bearings calculation, *Journal of Tribology* 119 (1997) 851–858.